Journal of Bioscience and Bioengineering
VOL. 128 No. 5, 585–592, 2019

ELSEVIER

www.elsevier.com/locate/jbiosc

Effects of rubber elongation factor and small rubber particle protein from rubber-producing plants on lipid metabolism in *Saccharomyces cerevisiae*

Saki Yokota and Takeshi Gotoh*

Department of Materials Science, Applied Chemistry Course, Graduate School of Engineering Science, Akita University, 1-1 Tegata Gakuen-machi, Akita City, Akita 010-8502, Japan

Received 7 November 2018; accepted 20 April 2019
Available online 20 May 2019

The common proteins rubber elongation factor (REF) and small rubber particle protein (SRPP) are associated with *Hevea brasiliensis* (Hb) rubber particles. They are involved in the stability of rubber particles and natural rubber biosynthesis. Recently, we cloned cDNAs encoding REF and SRPP from laticifers of *Ficus carica* (Fc). In the present study, we overexpressed REF/SRPPs (HbREF, FcREF, and FcSRPP) in *Saccharomyces cerevisiae* in anticipation of future rubber biosynthesis in recombinant yeast. The proteins were localized in the endoplasmic reticulum and lipid droplets (LDs), and affected LD morphology. Furthermore, their overexpression resulted in an accumulation of neutral lipids and a decrease in yeast cell size. This suggests that REF/SRPPs affect lipid metabolism and lead to a decline in the phospholipid content of yeast. We also found that expression of these proteins induced accumulation of steryl esters and triacylglycerols in yeast. This suggests that the coexpression of REF/SRPPs with key enzymes for the biosynthesis of target lipids in yeast is a promising way of increasing production of important lipids like triacylglycerols and terpenes, and that a protein complex consisting of *cis*-prenyltransferase (CPT), CPT-like protein, and REF/SRPPs for rubber biosynthesis could be reconstituted on yeast lipid droplets.

[**Key words:** *Hevea brasiliensis*; *Ficus carica*; Natural rubber latex proteins; Yeast lipid droplet; Lipid accumulation]

Natural rubber (NR or *cis*-1,4-polyisoprene) is an important biopolymer used in the production of rubber products such as vehicle tires, and the primary commercial source is the rubber tree *Hevea brasiliensis*. NR is present in plant laticifer cells as rubber particles, which are composed of a hydrophobic polyisoprene core and a surrounding monolayer membrane of phospholipids and proteins. Rubber elongation factor (REF) and small rubber particle protein (SRPP) are the major proteins associated with rubber particles in *Hevea* (1,2). Rubber transferase (*cis*-prenyl transferase, CPT), which catalyzes the *cis*-condensation of isopentenyl diphosphate with short-chain prenyl diphosphates such as farnesyl diphosphate, also binds to rubber particles (3,4). Two cDNAs encoding CPT (termed HRT1 and HRT2) were cloned from *Hevea* latex by Asawatreratanakul et al. (5). Recently, homologs of Nogo-B receptor, which interacts with CPT and increases its enzymatic activity, were identified from *Lactuca sativa* (*Lettuce*) latex and *Hevea* latex and termed CPT-like proteins 1 and 2 (CPTL1 and CPTL2) and HRT1–REF bridging protein (HRBP), respectively (6,7). Yamashita et al. (7) reported that *Hevea* rubber particles, whose CPT activity was almost abolished by washing with a detergent-containing buffer, restored their enzymatic activity via co-reconstitution of HRT1, HRBP, and *H. brasiliensis* REF (HbREF) on their outer membranes.

REF and SRPPs are homologs that share a common REF domain (Pfam protein family database accession number 05755), but their functions have not yet been fully elucidated. It has been suggested that HbREF stabilizes washed rubber particles (WRPs), and that coexpression of HbREF and HRBP stabilizes HRT1 on WRPs (7). On the other hand, Brown et al. (8) reported that coexpression of *H. brasiliensis* SRPP (HbSRPP) and HRBP displaced HRT2 (also known as CPT6) from the cytosol to the endoplasmic reticulum (ER) or plasma membrane (PM), but that HRT2 was unlikely to be stabilized by coexpression of HbSRPP and HRBP. Furthermore, in *Taraxacum brevicorniculatum*, which is another rubber-producing plant, SRPP (TbSRPP)-RNAi transgenic lines exhibited a reduction in dry rubber content and an aggregation and partial fusion of their rubber particles at pH 7.2 (9). Meanwhile, a recent study by Laibach et al. (10) reported that transiently expressed TbSRPPs in *Nicotiana benthamiana* were located mainly on lipid droplets (LDs) and the ER, and increased the number or size of LDs. Moreover, this paper indicated that the addition of TbSRPPs to artificial poly(*cis*-1,4-isoprene) bodies resulted in a narrowing of their size distribution. REF/SRPP-family proteins have been found not only in natural rubber-producing plants, but also in non-rubber-producing plants. In *Arabidopsis thaliana*, constitutive overexpression of SRPP homologs resulted in increased numbers of large LDs in post-germination seedlings (11). Gidda et al. (12) termed these proteins LD-associated proteins 1–3 (LDAP1, LDAP2, and LDAP3) and determined that overexpression of LDAPs resulted in an increase in LDs and the neutral lipid content of *Arabidopsis* leaves. Thus, it is suggested that REF/SRPP-family proteins have roles in maintaining the structure of rubber particles or LDs and in facilitating the formation of a rubber biosynthesis protein complex on rubber particles.

* Corresponding author. Tel./fax: +81 18 889 2741.
E-mail address: tgotoh@gipc.akita-u.ac.jp (T. Gotoh).

1389-1723/$ – see front matter
https://doi.org/10.1016/j.jbiosc.2019.04.018

LDs have a structure similar to rubber particles, consisting of a neutral lipid core covered by a monolayer membrane of phospholipids and proteins, and as mentioned above, rubber-associated proteins were located mainly on LDs and the ER in a non-rubber producing model plant. Qu et al. (6) reported that coexpression of CPT and CPTL from lettuce in *Saccharomyces cerevisiae* (yeast) facilitated the colocalization of these two proteins in the ER and LDs. These findings led us to hypothesize that NR can be biosynthesized in yeast by reconstituting a protein complex consisting of CPT, CPTL, and REF/SRPP-family proteins for rubber biosynthesis in yeast LDs. Prior to this study, the subcellular localization of recombinant REF/SRPPs in yeast was unknown.

In the present study, we expressed *Ficus carica* REF/SRPPs (FcREF, and FcSRPP), which were cloned in our previous study (13), and HbREF in yeast. We then examined their subcellular localization and effects on LD formation and lipid accumulation. Our results showed that expression of REF/SRPPs affects lipid metabolism in yeast.

MATERIALS AND METHODS

Construction of plasmids A vector backbone (GAP promoter-inserted YEp352, YEp352-pGAP) was linearized by inverse PCR using CloneAmp HiFi PCR Premix (Takara Bio, Shiga, Japan). HbREF, FcREF, and FcSRPP-coding regions were amplified by PCR using KOD-plus-Neo DNA polymerase and pCold-HbREF, -REF/SRPP-1 (FcREF), and -REF/SRPP-2 (FcSRPP) from our previous study (13) as templates. To add a FLAG-tag sequence at the C-terminus of the HbREF, FcREF, and FcSRPP sequences, PCR was carried out using 3′ specific primers, each containing the FLAG-tag sequence. Subsequently, a second PCR was performed using specific primers, each containing a 15 bp extension homologous to vector ends. The amplified DNA fragments were inserted into the linearized YEp352-pGAP using the In-Fusion HD Cloning Kit (Takara Bio) to generate YEp352-HbREF, YEp352-FcREF, and YEp352-FcSRPP.

We also constructed a plasmid for expression of Sec63 tagged at the C-terminus of enhanced green fluorescent protein (EGFP) in order to use as an ER marker. Yeast SNY9 (MATα, mfα1::ADE2, mfα2::TRP1, bar1::HIS3, ade2, trp1, his3, leu2, ura3, lys2) was cultured in YPD medium, and total RNA was isolated by using the AquaPure RNA isolation kit (Bio-Rad, Hercules, CA, USA). Sec63 gene was prepared by RT-PCR with specific primers using a Superscript IV One-Step RT-PCR System (Invitrogen, Carlsbad, CA, USA). The PCR product was treated with RNase A (Takara Bio) and purified using FastGene Gel/PCR Extraction Kit (Nippon Genetics, Tokyo, Japan). A second PCR was carried out using the purified DNA as a template and 5′ and 3′ specific primers containing 15 bp extensions homologous to 3′-end of linearized pBEVY-L and 5′-end of EGFP gene, respectively. A 15 bp extension homologous to 5′-end of the linearized vector was added to the 3′-end of the EGFP sequence by PCR using pCold I-EGFP as a template and 3′ specific primer containing the extension sequence. The resulting Sec63 and EGFP cDNAs were cloned downstream to a GAP promoter of the linearized pBEVY-L using In-Fusion HD Cloning Kit (Takara Bio) to generate pBEVY-L-Sec63-EGFP. A complete list of oligonucleotide primers used for the generation of DNA constructs in this study is shown in Supplementary Table S1.

Yeast transformation and growth conditions Yeast SNY9 was used as a host strain. The yeast strain was transformed with YEp352-HbREF, YEp352-FcREF, YEp352-FcSRPP, or an empty vector (mock) using the *S. cerevisiae* Direct Transformation Kit Wako (Wako, Tokyo, Japan), plated onto SD-Ura plates, and incubated for 3 d at 30°C. For costaining the REF/SRPPs and ER, the cells were further cotransformed with pBEVY-L-Sec63-EGFP and plated onto SD-Leu-Ura plated. These transformed cells were cultured in SD-Ura/-Leu-Ura medium at 30°C until they reached an absorbance at 600 nm (OD_{600}) of approximately 1.5–2.5, then diluted in additional SD-Ura/-Leu-Ura medium to an OD_{600} of 0.1 and cultured at 30°C.

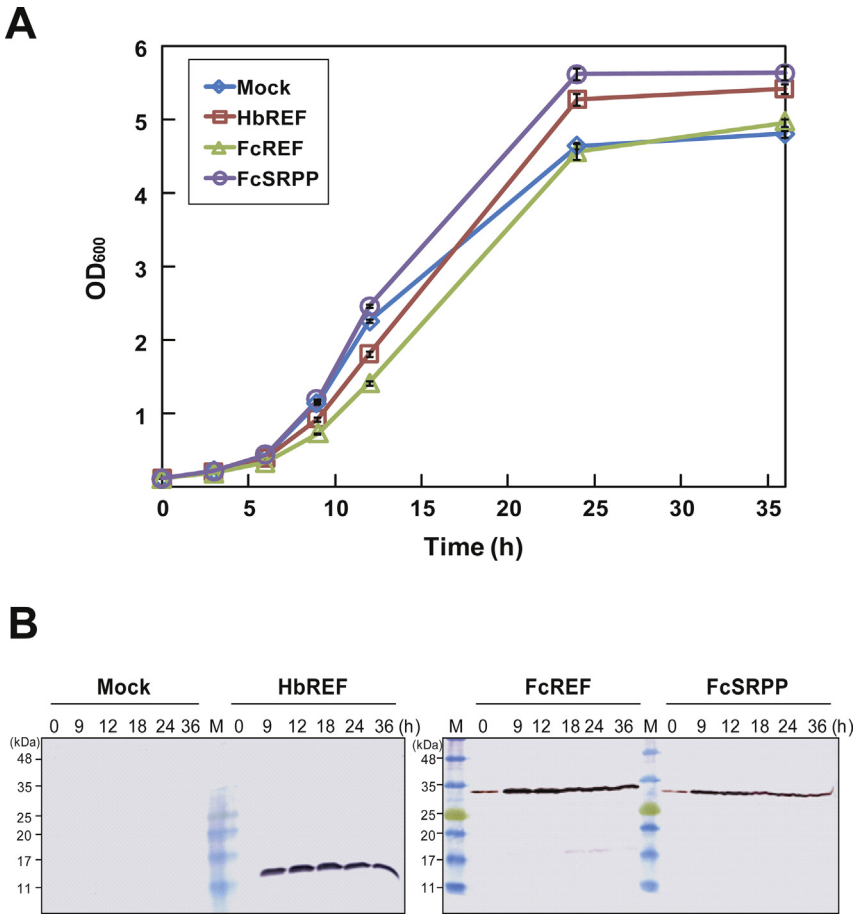

FIG. 1. Growth of REF/SRPP-expressing yeast cells and expression of recombinant proteins. (A) Growth curve of recombinant yeast strains. Yeast cells (SNY9) were transformed with YEp352-HbREF (HbREF), YEp352-FcREF (FcREF), YEp352-FcSRPP (FcSRPP), and YEp352 empty vector (Mock). The recombinant cells were grown in SD-Ura medium at 30°C for 36 h. At the time points indicated, aliquots of the culture were taken and their OD_{600} was measured. (B) Anti-FLAG Western blot analysis of HbREF (16 kDa), FcREF (29 kDa), and FcSRPP (28 kDa) expression.

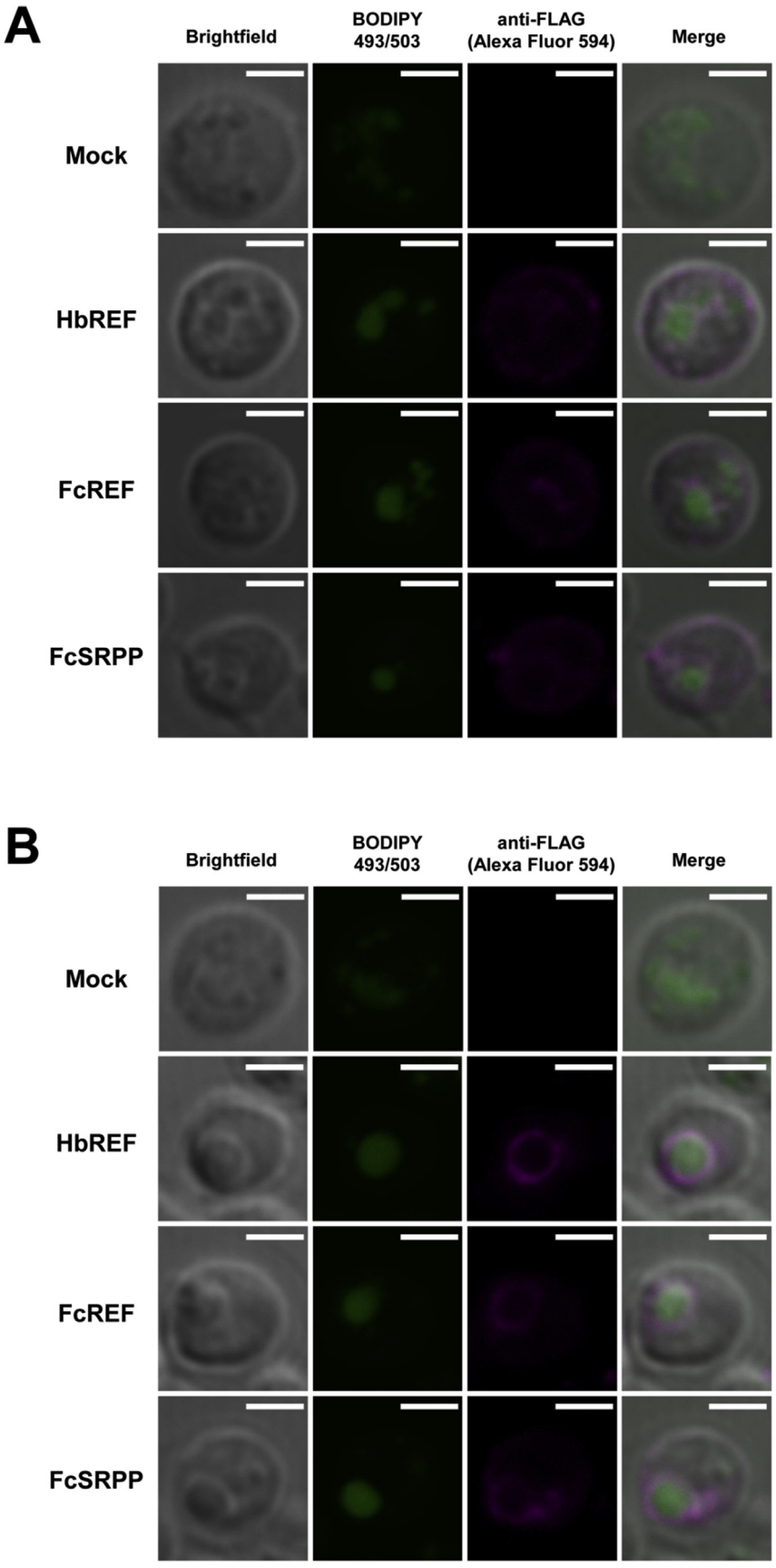

FIG. 2. Subcellular localization of HbREF, FcREF, and FcSRPP in yeast cells in an exponential growth phase. The recombinant cells were grown in SD-Ura medium at 30°C for 12 h, and were then costained with BODIPY 493/503 and anti-FLAG antibody, followed by Alexa Fluor 594-labeled secondary antibody. Two types of REF/SRPPs localization can be seen: (A) distribution like typical ER and (B) distribution surrounding a large LD. Scale bars: 2 μm.

Immunoblot analysis Proteins were extracted from yeast cells using the alkaline lysis-modified procedure (14). Resulting supernatant fractions were run using SDS-PAGE. The proteins were transferred from the gel to nitrocellulose membranes (Bio-Rad). As the primary antibody, mouse anti-DDDDK-tag antibody (MBL, Nagoya, Japan) was used at a 1250-fold dilution in PBS (pH 7.4). As the secondary antibody, goat anti-mouse IgG H&L (heavy and light chain)-alkaline phosphatase conjugate (Cosmo Bio, Tokyo, Japan) was used at a 2000-fold dilution in blocking solution containing 5% skim milk.

Immunofluorescence staining Immunofluorescence analysis of the yeast cells was performed according to Robinson et al. (15) with slight modification. Briefly, yeast cells were fixed with 3.6% formaldehyde. Cells were washed with 0.1 M KPO_4 buffer (pH 7.5), resuspended in 1 M sorbitol containing 75 μg/ml Zymolyase-20 T and 0.002% 2-mercaptoethanol, incubated at 30°C for 40 min, then 0.2% SDS was added and the samples were placed in an ice bath for 10 min. The resulting spheroplasts were washed three times with G1T (1% gelatin, 0.5 mg/ml BSA, 150 mM NaCl, 50 mM HEPES (pH 7.5), 0.1% Tween 20, 1 mM NaN_3). The cells were incubated in G3T (3% gelatin, 0.5 mg/ml BSA, 150 mM NaCl, 50 mM HEPES (pH 7.5), 0.1% Tween 20, 1 mM NaN_3) at 25°C for 1 h, then with anti-DDDDK-tag antibody (MBL) for 1 h, and then washed with G1T three times. Next, cells were stained with Goat Anti-Mouse IgG H&L (Alexa Fluor 594, Abcam, Cambridge, MA, USA) for 30 min and washed with G1T five times. Subsequently, the cells' LDs were stained with BODIPY 493/503 (5 μM; Thermo Fisher Scientific, Waltham, MA, USA) for 5 min and washed with 0.1 M KPO_4 buffer (pH 7.5) three times. The resulting stained cells were resuspended in 10 mM HEPES (pH 7.5) containing 50% glycerol. Finally, the cells were analyzed with a confocal laser scanning microscope (LSM 780, Carl Zeiss, Oberkochen, Germany).

Quantification of cellular lipid accumulation After cultivation in SD-Ura medium, recombinant cells were collected by centrifugation and fixed with 3.6% formaldehyde. The cell suspensions were diluted in 0.1 M KPO_4 buffer (pH 7.5) to an OD_{600} of approximately 0.5. Aliquots (1 ml) of this cell suspension were stained with BODIPY 493/503 (5 μM; Thermo Fisher Scientific) and washed with 0.1 M KPO_4 buffer (pH 7.5) three times. Flow cytometry analysis of BODIPY 493/503-stained cells and unstained cells was performed using a BD FACSAria (BD Biosciences, San Jose, CA, USA). Ten thousand events were acquired per sample, and delta mean fluorescence intensity (ΔMFI) was calculated by subtracting the mean fluorescence intensity of the unstained cell sample from the mean fluorescence intensity of the stained cell sample using the BD FACS-Diva software (BD Biosciences).

Lipid analysis Lipids were prepared as described previously (16). In brief, recombinant cells in an exponential growth phase (12 h) were resuspended in chloroform/methanol (2:1 v/v) and lysed with zirconia beads (0.3 mm in diameter). Sodium chloride solution was added and then the mixture was centrifuged. The organic (lower) phase was collected and dried by evaporation under a gentle stream of nitrogen, and the lipids were dissolved in chloroform/methanol. For thin-layer chromatography (TLC) analysis of neutral lipids, the lipids were applied to a silica gel 60 TLC plate (Merck, Darmstadt, Germany). Five micrograms of cholesterol (Sigma–Aldrich, St. Louis, MO, USA) and cholesterol oleate (Tokyo Chemical Industry, Tokyo, Japan) and 20 μg of triolein (Tokyo Chemical Industry) were spotted onto the plate as authentic standards. A two-step separation system was performed as described previously (17). Ergosterol (ERG) and steryl esters (SEs) were stained with an $MnCl_2$ solution and heated at 100°C for 15 min, and triacylglycerols (TAGs) were stained by iodine vapor. The plates were scanned and quantified using ImageJ software. To normalize the relative lipid contents with cellular metabolic activity, MTT assay was performed using recombinant cells in exponential growth phase (cultured for 9, 12, 15, 18 h) with Cell Proliferation kit I (MTT) (Roche, Nutley, NJ, USA).

Fluconazole sensitivity assay Yeast cells were grown in SD-Ura medium to an exponential growth phase, and then cell density was adjusted to an OD_{600} of 0.1. Cells were serially 10-fold diluted and 5 μL was spotted onto YPD agar plates with or without fluconazole (50 μg/ml).

RESULTS

Subcellular localization of REF/SRPPs in yeast, and their effect on lipid droplet morphology To investigate the subcellular localization of HbREF, FcREF, and FcSRPP in yeast, the cDNAs were expressed constitutively under the control of a GAP promoter in the YEp352 vector. The recombinant cells were cultured in SD-Ura medium to a stationary growth phase at 30°C for 36 h, and cell growth was monitored by measuring the OD_{600}. As shown in Fig. 1A, the growth of the HbREF- and FcREF-expressing cells was slower than that of the mock and FcSRPP-expressing cells, and

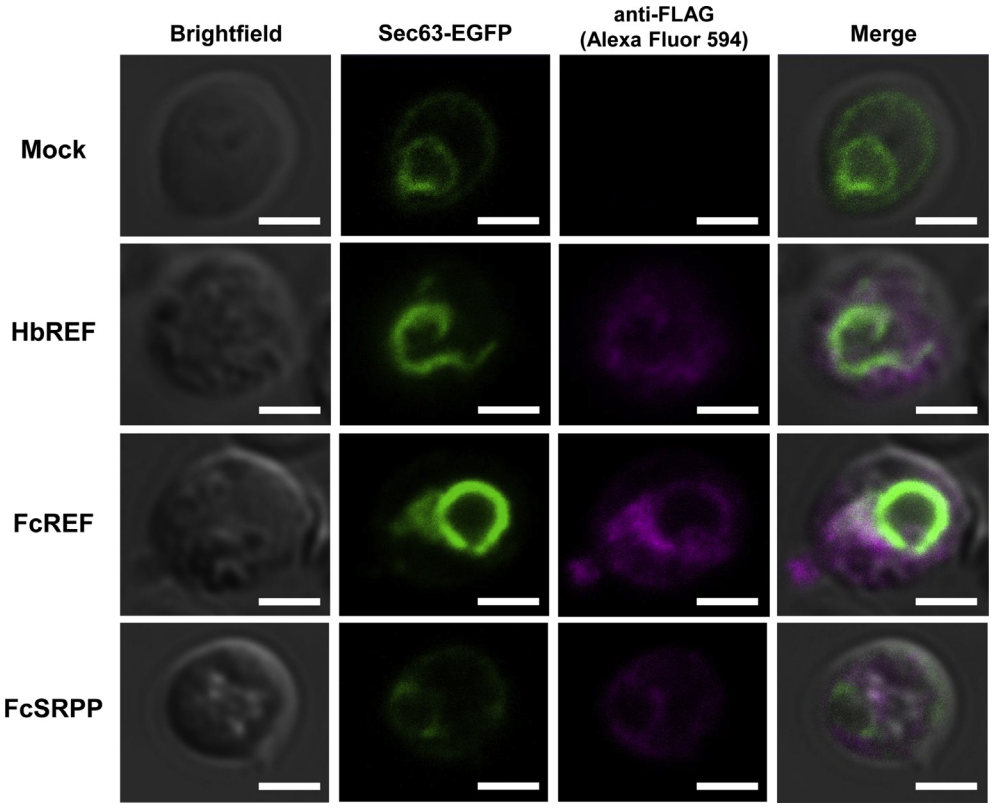

FIG. 3. Subcellular localization of HbREF, FcREF, FcSRPP and ER marker Sec63-EGFP in yeast cells in an exponential growth phase. Cells coexpressing REF/SRPP and Sec63-EGFP were analyzed. Scale bars: 2 μm.

the HbREF- and FcSRPP-expressing cells were more abundant than the mock and FcREF-expressing cells.

Volumetric expression of HbREF, FcREF, and FcSRPP was examined using densitometric analysis following Western blot with an antibody against FLAG-tag, which was engineered at the C-terminus of these proteins (Fig. 1B). The recombinant proteins were observed at their respective expected molecular weights. Their expression levels were apparently maximized at 12 h during an exponential growth phase, and then gradually decreased while the cells continued to grow until 24 h.

Immunofluorescence microscopy was performed on the cells at 12 h in an exponential growth phase, using Alexa Fluor 594-conjugated goat anti-mouse IgG antibody, to determine the intracellular localization of the recombinant proteins. The immunofluorescence signals revealed that these recombinant proteins had two distinct localization patterns in common: (i) dotted signals assembling in close proximity to LDs, which was costained with LD dye (BODIPY 493/503), and the PM (Fig. 2A), and (ii) a marked ring-like signal encircling a single large LD (Fig. 2B). The former looks like typical ER patterns (known as nuclear ER and cortical ER) in yeast (18). To visualize the ER, the REF/SRPP-expressing and mock cells were transformed with pBEVY-L-Sec63-EGFP for coexpressing EGFP-labeled Sec63, which has been used extensively as an ER marker (19–21). Since cell growth was significantly delayed due to the cotransformation (Fig. S1), immunofluorescence microscopy was performed on the cells at 30–36 h in the an exponential growth phase. Although the signals of these fluorescence markers were not strongly determined together in every cell, the REF/SRPP signal coincided with the Sec63 signal in cells that the signals were both significantly determined (Fig. 3). REF/SRPP signals that unmatched Sec63 signal may be adjacent to LDs because REF/SRPPs were localized also around LDs (Fig. 2). Thus, these results suggest that REF/SRPPs localize on the ER and LDs in yeast, as in *N. benthamiana* leaves (8,10,11). The immunofluorescence microscopy analysis of the cells coexpressing Sec63 also showed that the ER having HbREF and FcREF were deformed extremely (Fig. 3). This may be attributed to enhanced overexpression of REF and Sec63 in the ER.

Expression of REF/SRPP-family proteins reportedly affects LD morphology in plant tissue (10,11). As shown in Fig. 2, the LDs in REF/SRPP-expressing cells are much larger than those in the mock cells. We analyzed the size of the LDs in recombinant yeast cells during the exponential growth phase by measuring the volume of three-dimensional LD images, reconstructed using Imaris image analysis software (Bitplane, Zurich, Switzerland), to determine whether the size distribution of the LDs varied with the type of REF/SRPPs that was localized on the LDs. However, there were no clear differences among their size distributions (data not shown), probably because closely adjacent LDs were recognized as a single LD by the image analysis software. Large LDs were observed in some of the many mock cells (Fig. 2B, mock). However, the large LDs in mock cells were probably clusters of small LDs, because their shapes were extremely distorted in comparison to the spherical shape observed in REF/SRPP-expressing cells, and the fluorescent signals were sparsely dotted. These findings suggest that expression of HbREF, FcREF, and FcSRPP, which were localized on LDs, affected the morphology of the LDs in yeast cells in the same way as in plant tissue.

REF/SRPP-induced lipid accumulation in yeast LDs In addition to the increase in the size of LDs, the BODIPY 493/503 fluorescence intensity of REF/SRPP-expressing cell lines appeared to increase relative to that of mock cells. We next investigated whether REF/SRPP expression could lead to the accumulation of

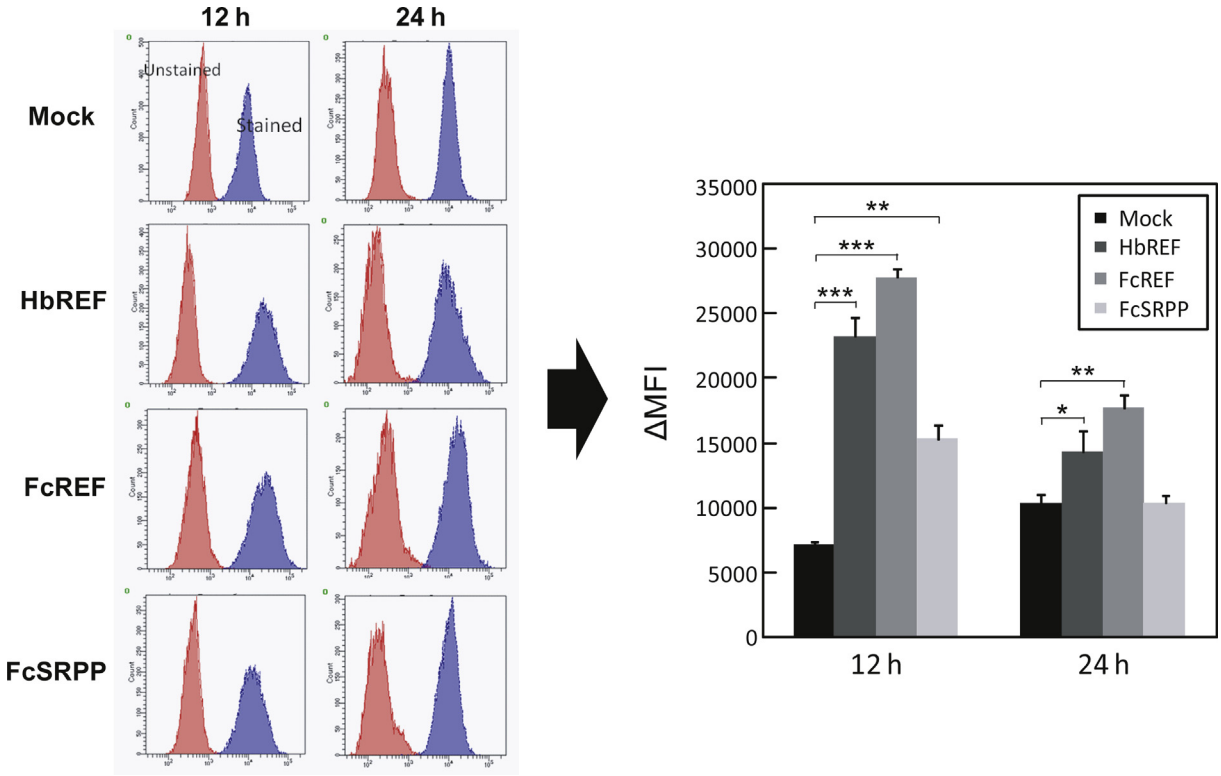

FIG. 4. Comparison of LD level among REF/SRPP-expressing yeast cells. Flow cytometry analysis was performed for REF/SRPP-expressing cells in an exponential growth phase. Representative flow cytometry histograms of fluorescence signal intensity were shown for BODIPY 493/503-stained (blue) and unstained cells (red) (left panel). Bar graph represented the ΔMFIs of the BODIPY fluorescence signal in the recombinant cells (right panel). ΔMFIs were calculated using the equation $\Delta MFI = (MFI_{stained\ cells} - MFI_{unstained\ cells})$. Data presented are results from three independent experiments, with error bars representing standard deviation. *P* values were calculated using a *t*-test (*, $p < 0.1$; **, $p < 0.01$; ***, $p < 0.001$).

TABLE 1. Relative size of the recombinant yeast cells.

	Mock	HbREF	FcREF	FcSRPP
12 h	128.3 ± 1.9	71.5 ± 0.7	92.7 ± 0.6	70.9 ± 0.3
24 h	152.0 ± 2.3	100.8 ± 1.9	94.7 ± 1.8	89.8 ± 1.0

The FSC-A of 10,000 events of REF/SRPP-expressing cells was obtained via flow cytometry analysis. Values are means of three independent runs with 10,000 events each, ± standard deviations (SD).

intracellular lipids. The fluorescence intensity of BODIPY 493/503-stained and -unstained (negative control) cells in exponential growth (12 h) and stationary (24 h) phases was measured using flow cytometry, and delta mean fluorescence intensity (ΔMFI) values, i.e., the difference in MFI between BODIPY 493/503-stained cells and unstained control cells, were calculated (Fig. 4). In the exponential growth phase, the fluorescence intensity of REF-expressing cells was 3.4–3.7 times higher than that of mock cells. For SRPP-expressing cells, the fluorescence level was more than twice as high as that of mock cells. However, these significant increases were attenuated in the stationary phase. During culture, the glucose concentration of the medium decreased from an initial 2% to below 0.3% (data not shown). The reduction in fluorescence intensity may therefore be attributable to lipolytic responses to starvation. In contrast to the LDs, the REF/SRPP-expressing cells were smaller than the mock cells (Table 1). According to Rao et al. (22), yeast cell size is dictated by the quantity of phospholipids and not correlated with the quantity of storage lipids. Our results suggest that expression of REF/SRPPs led to a decline in phospholipids content as well as an accumulation of storage lipids, TAGs and/or SEs, in yeast.

At 12 h, when the LDs were maximized during the exponential growth phase, the accumulation of neutral lipids in the yeast cells was further examined via TLC analysis. Based on culture volume, the quantity of neutral lipids in the REF/SRPP-expressing cells was rarely different from that in the mock cells (Fig. 5A, B, left panel). On an OD_{600} basis, SEs and ERG were enhanced in REF/SRPP-

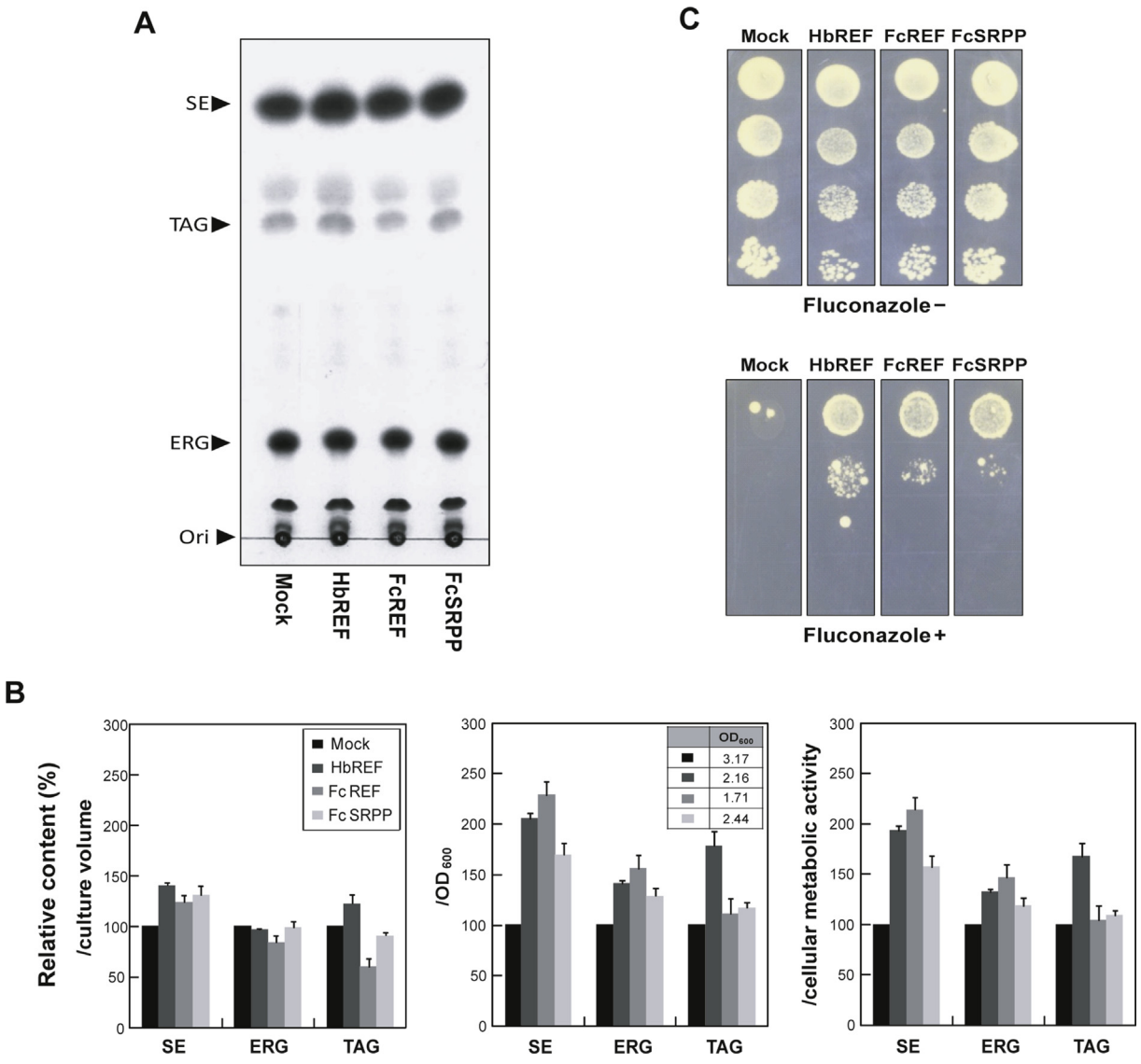

FIG. 5. Lipid analysis of REF/SRPP-expressing cells in an exponential growth phase. (A) Lipids were extracted from the recombinant cells during an exponential growth phase and an equal volume of lipid extracts was separated using TLC. Standard mixture was composed of cholesterol, triolein, cholesterol oleate. (B) The relative content of each category of neutral lipid was analyzed using densitometric scanning. The values of relative lipid content were normalized by culture volume (left panel), OD_{600} (middle panel), and cellular metabolic activity (right panel). The box in middle panel shows OD_{600} values of the 12 h cultures. ERG, ergosterol; TAG, triacylglycerols; SE, steryl esters. Data presented are results from three independent experiments with error bars representing standard deviation. (C) Resistance of the recombinant cells to fluconazole, an antifungal agent. Tenfold serial dilutions of yeast cells were spotted on YPD plates with or without fluconazole (50 μg/ml).

expressing cells and TAGs were enhanced only in HbREF-expressing cells (Fig. 5B, middle panel). However, the OD_{600} values did not reflect cell numbers because the expression of REF/SRPPs affected cell size. We therefore examined metabolic activity of the cells by MTT assay, and evaluated the lipid accumulation based on the cellular metabolic activity (Fig. 5B, right panel), using correlation curve between OD_{600} and MTT absorbance (Fig. S2). SEs and ERG were enhanced in REF/SRPP-expressing cell, and TAGs were elevated in HbREF-expressing cells, even though the individual cells were smaller. It has been reported that overexpression of *Arabidopsis* LDAPs (SRPP homologs) results in an increase in the neutral lipid content of *Arabidopsis* leaves (12). Our results demonstrate that REF/SRPPs cause neutral lipids to accumulate in LDs in yeast as well. This was particularly the case for the SEs. We examined the resistance of the REF/SRPP-expressing yeast strains to fluconazole, which acts as an antifungal agent by inhibiting ERG biosynthesis. Each of the recombinant yeast strains acquired resistance to fluconazole (Fig. 5C). This suggests that sterol (ERG) synthesis was promoted in the REF/SRPP-expressing cells because sterols are esterified and stored in LDs. Fig. 6 illustrates the changes in yeast lipid metabolism caused by expression of REF/SRPPs from rubber-producing plants that are suggested by these findings. When REF/SRPP-family proteins are expressed in yeast, they are localized on the ER and LDs, leading to a promotion of neutral lipids synthesis, as well as a suppression of phospholipid synthesis.

DISCUSSION

Several studies have reported that recombinant HbREF polymerizes as an amyloid and quickly forms large aggregates, and that HbSRPP auto-assembles into more-globular stable nanomultimers in PBS (23,24). In addition, HbREF and HbSRPP may interact with each other (24). Wadeesirisak et al. (25) suggested that the interaction between recombinant HbREF and a lipid monolayer consisting of neutral lipids extracted from *Hevea* latex promoted the aggregation of HbREF into an amyloid form. We previously reported that recombinant FcREF and FcSRPP tended to aggregate in PBS, though the growth rate and size of FcREF aggregates were distinctly different from those of FcSRPP aggregates (13). *Arabidopsis* SRPP homologs (SRP1–3) have polymerization properties *in vivo* and *in vitro* (11). Meanwhile, there are some reports that LDs are enlarged in REF/SRPP-expressing cells. The *T. brevicorniculatum* SRPP homolog TbSRPP5, for example, was found to enlarge LDs in *N. benthamiana* leaves (10), and the *Arabidopsis* SRPP homologs, stress-related protein (SRP1–3, also known as LDAP1–3) were found to increase the numbers of large LDs in postgermination seedlings (11). Similarly, the present study demonstrated that expression of REF/SRPPs from *H. brasiliensis* or *F. carica* in yeast results in enlarged LDs. Kim et al. (11) proposed that self- or hetero-aggregation of REF/SRPP-family proteins is thought to be involved in the regulation of LD size. The present study found that REF/SRPP-expressing cells contained a larger quantity of neutral lipids than mock cells at 12 h during the exponential growth phase. One possible explanation for this is that the decrease in the specific surface area of larger LDs contributes to the reduced access of lipases to internal lipids, as previously suggested (26). The high neutral-lipid content observed in the exponential growth phase decreased gradually during the stationary phase. This may have been caused by LD autophagy in response to starvation (27), in order to regenerate and reuse acetyl-CoA. Accordingly, the REF/SRPPs would also have degraded gradually (Fig. 1B). If that were the case, the LD degradation could be prevented by using a fed-batch culture with glucose concentration control. Furthermore, LDs with coexpressed REF/SRPPs and key enzymes for lipid synthesis on them could be used for the enhanced production of useful lipids such as TAGs and terpenes in yeast-based synthetic biology.

HbREF, FcREF, and FcSRPP showed high homology in their primary structure with each other, though FcREF was similar to HbREF in aggregation property but extremely different from FcSRPP (13). In the present study, no apparent difference was observed in LD size and/or lipid accumulation between REF- and SRPP-expressing

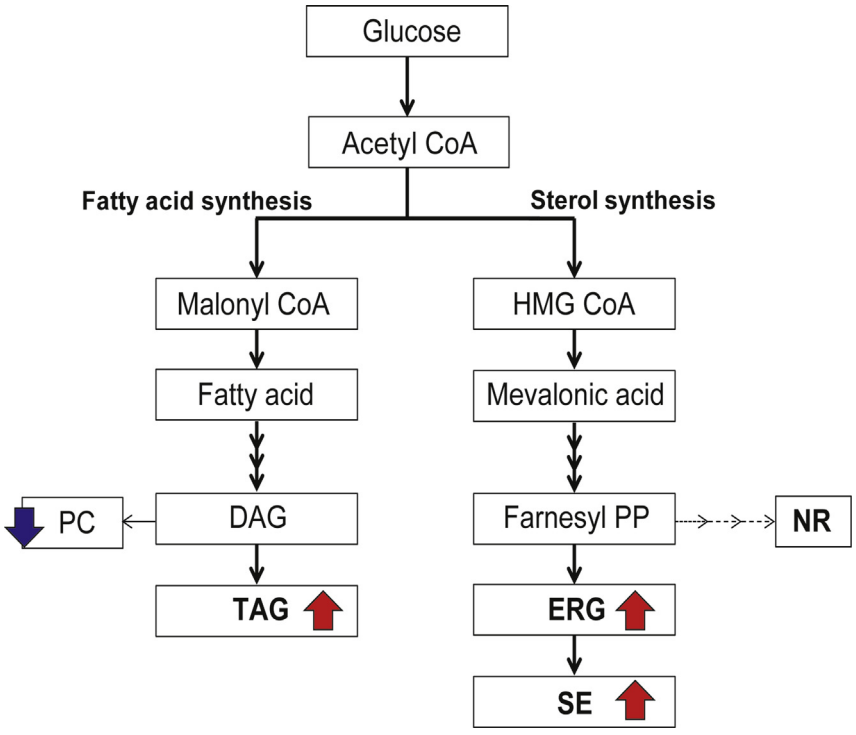

FIG. 6. Lipid metabolism induced by the expression of REF/SRPP-family proteins. Expression of REF/SRPP-family proteins expedited not only TAG synthesis but also ERG synthesis and SE accumulation. Conversely, phospholipid synthesis was limited, and consequently the REF/SRPP-expressing cells were smaller than the mock cells.

strains. Meanwhile, our immunofluorescence microscopy analysis showed that the ER having HbREF and FcREF were deformed extremely (Fig. 3). This may be caused by co-overexpression of REF and Sec63 in the ER. The influence of REF/SRPP expression on ER morphology should be in detail examined in the next study.

Contrary to the positive correlation between REF/SRPP expression and LD enlargement, a recent study reported that LDAP1 knockout in senescing *Arabidopsis* leaves increased the variability of LD size, with some noticeably larger LDs appearing (28). In addition, the *Arabidopsis* LDAP-interacting protein (LDIP) was identified, and LDIP disruption led to a progressively greater variation in LD size, with larger LDs developing in the KO leaves (26). Thus, further study is necessary to determine whether HbREF, FcREF, and FcSRPP interact with yeast LD proteins.

In conclusion, the present study has demonstrated that, when REF/SRPPs from rubber-producing *H. brasiliensis* and *F. carica* plants were expressed in yeast, they were located on the ER and LDs, and affected lipid metabolism. This suggests that the proteins CPT, CPTL, and REF/SRPP, which are associated with NR biosynthesis, are likely to colocalize on yeast LDs to generate a protein complex. We found that the expression of REF/SRPPs facilitates neutral lipids accumulation in yeast. Since NR is an isoprenoid polymer, limitation of the ERG-biosynthesis pathway and overexpression of a protein complex consisting of CPT, CPTL, and REF/SRPP would be favorable for achieving the biosynthesis and accumulation of NR in yeast.

Supplementary data to this article can be found online at https://doi.org/10.1016/j.jbiosc.2019.04.018.

ACKNOWLEDGMENTS

This work was supported in part by JSPS KAKENHI Grant Number 16K06865.

References

1. **Dennis, M. S. and Light, D. R.:** Rubber elongation factor from *Hevea brasiliensis*. Identification, characterization, and role in rubber biosynthesis, J. Biol. Chem., **264**, 18608–18617 (1989).
2. **Oh, S. K., Kang, H., Shin, D. H., Yang, J., Chow, K. S., Yeang, H. Y., Wagner, B., Breiteneder, H., and Han, K. H.:** Isolation, characterization, and functional analysis of a novel cDNA clone encoding a small rubber particle protein from *Hevea brasiliensis*, J. Biol. Chem., **274**, 17132–17138 (1999).
3. **Archer, B. L. and Cockbain, E. G.:** Rubber transferase from *Hevea brasiliensis* latex, pp. 476–480, in: Archer, B. L., Cockbain, E. G., and Clayton, R. B. (Eds.), Methods in enzymology, vol. 15. Academic Press (1969).
4. **Cornish, K.:** The separate roles of plant cis and trans prenyl transferases in *cis*-1,4-polyisoprene biosynthesis, Eur. J. Biochem., **218**, 267–271 (1993).
5. **Asawatreratanakul, K., Zhang, Y. W., Wititsuwannakul, D., Wititsuwannakul, R., Takahashi, S., Rattanapittayaporn, A., and Koyama, T.:** Molecular cloning, expression and characterization of cDNA encoding *cis*-prenyltransferases from *Hevea brasiliensis*. A key factor participating in natural rubber biosynthesis, Eur. J. Biochem., **270**, 4671–4680 (2003).
6. **Qu, Y., Chakrabarty, R., Tran, H. T., Kwon, E. J., Kwon, M., Nguyen, T. D., and Ro, D. K.:** A lettuce (*Lactuca sativa*) homolog of human Nogo-B receptor interacts with *cis*-prenyltransferase and is necessary for natural rubber biosynthesis, J. Biol. Chem., **290**, 1898–1914 (2015).
7. **Yamashita, S., Yamaguchi, H., Waki, T., Aoki, Y., Mizuno, M., Yanbe, F., Ishii, T., Funaki, A., Tozawa, Y., Miyagi-Inoue, Y., and other 3 authors:** Identification and reconstitution of the rubber biosynthetic machinery on rubber particles from *Hevea brasiliensis*, eLife, **5**, e19022 (2016).
8. **Brown, D., Feeney, M., Ahmadi, M., Lonoce, C., Sajari, R., Di Cola, A., and Frigerio, L.:** Subcellular localization and interactions among rubber particle proteins from *Hevea brasiliensis*, J. Exp. Bot., **68**, 5045–5055 (2017).
9. **Hillebrand, A., Post, J. J., Wurbs, D., Wahler, D., Lenders, M., Krzyzanek, V., Prufer, D., and Gronover, C. S.:** Down-regulation of small rubber particle protein expression affects integrity of rubber particles and rubber content in *Taraxacum brevicorniculatum*, PLoS One, **7**, e41874 (2012).
10. **Laibach, N., Schmidl, S., Muller, B., Bergmann, M., Prufer, D., and Schulze Gronover, C.:** Small rubber particle proteins from *Taraxacum brevicorniculatum* promote stress tolerance and influence the size and distribution of lipid droplets and artificial poly(*cis*-1,4-isoprene) bodies, Plant J. Cell Mol. Biol., **93**, 1045–1061 (2018).
11. **Kim, E. Y., Park, K. Y., Seo, Y. S., and Kim, W. T.:** Arabidopsis small rubber particle protein homolog SRPs play dual roles as positive factors for tissue growth and development and in drought stress responses, Plant Physiol., **170**, 2494–2510 (2016).
12. **Gidda, S. K., Park, S., Pyc, M., Yurchenko, O., Cai, Y., Wu, P., Andrews, D. W., Chapman, K. D., Dyer, J. M., and Mullen, R. T.:** Lipid droplet-associated proteins (LDAPs) are required for the dynamic regulation of neutral lipid compartmentation in plant cells, Plant Physiol., **170**, 2052–2071 (2016).
13. **Yokota, S., Suzuki, Y., Saitoh, K., Kitajima, S., Ohya, N., and Gotoh, T.:** Cloning and aggregation characterization of rubber elongation factor and small rubber particle protein from *Ficus carica*, Mol. Biotechnol., **60**, 83–91 (2018).
14. **Von der Haar, T.:** Optimized protein extraction for quantitative proteomics of yeasts, PLoS One, **2**, e1078 (2007).
15. **Robinson, N. G., Guo, L., Imai, J., Toh, E. A., Matsui, Y., and Tamanoi, F.:** Rho3 of *Saccharomyces cerevisiae*, which regulates the actin cytoskeleton and exocytosis, is a GTPase which interacts with Myo2 and Exo70, Mol. Cell Biol., **19**, 3580–3587 (1999).
16. **Folch, J., Lees, M., and Sloane Stanley, G. H.:** A simple method for the isolation and purification of total lipides from animal tissues, J. Biol. Chem., **226**, 497–509 (1957).
17. **Connerth, M., Czabany, T., Wagner, A., Zellnig, G., Leitner, E., Steyrer, E., and Daum, G.:** Oleate inhibits steryl ester synthesis and causes liposensitivity in yeast, J. Biol. Chem., **285**, 26832–26841 (2010).
18. **Fehrenbacher, K. L., Davis, D., Wu, M., Boldogh, I., and Pon, L. A.:** Endoplasmic reticulum dynamics, inheritance, and cytoskeletal interactions in budding yeast, Mol. Biol. Cell, **13**, 854–865 (2002).
19. **Prinz, W. A., Grzyb, L., Veenhuis, M., Kahana, J. A., Silver, P. A., and Rapoport, T. A.:** Mutants affecting the structure of the cortical endoplasmic reticulum in Saccharomyces cerevisiae, J. Cell Biol., **150**, 461–474 (2000).
20. **Voeltz, G. K., Prinz, W. A., Shibata, Y., Rist, J. M., and Rapoport, T. A.:** A class of membrane proteins shaping the tubular endoplasmic reticulum, Cell, **124**, 573–586 (2006).
21. **Schuck, S., Prinz, W. A., Thorn, K. S., Voss, C., and Walter, P.:** Membrane expansion alleviates endoplasmic reticulum stress independently of the unfolded protein response, J. Cell Biol., **187**, 525–536 (2009).
22. **Rao, M. J., Srinivasan, M., and Rajasekharan, R.:** Cell size is regulated by phospholipids and not by storage lipids in *Saccharomyces cerevisiae*, Curr. Genet., **64**, 1071–1087 (2018).
23. **Berthelot, K., Lecomte, S., Estevez, Y., Coulary-Salin, B., Bentaleb, A., Cullin, C., Deffieux, A., and Peruch, F.:** Rubber elongation factor (REF), a major allergen component in *Hevea brasiliensis* latex has amyloid properties, PLoS One, **7**, e48065 (2012).
24. **Berthelot, K., Lecomte, S., Estevez, Y., Coulary-Salin, B., and Peruch, F.:** Homologous *Hevea brasiliensis* REF (Hevb1) and SRPP (Hevb3) present different auto-assembling, Biochim. Biophys. Acta, **1844**, 473–485 (2014).
25. **Wadeesirisak, K., Castano, S., Berthelot, K., Vaysse, L., Bonfils, F., Peruch, F., Rattanaporn, K., Liengprayoon, S., Lecomte, S., and Bottier, C.:** Rubber particle proteins REF1 and SRPP1 interact differently with native lipids extracted from *Hevea brasiliensis* latex, Biochim. Biophys. Acta Biomembr., **1859**, 201–210 (2017).
26. **Pyc, M., Cai, Y., Gidda, S. K., Yurchenko, O., Park, S., Kretzschmar, F. K., Ischebeck, T., Valerius, O., Braus, G. H., Chapman, K. D., Dyer, J. M., and Mullen, R. T.:** Arabidopsis lipid droplet-associated protein (LDAP) - interacting protein (LDIP) influences lipid droplet size and neutral lipid homeostasis in both leaves and seeds, Plant J. Cell Mol. Biol., **92**, 1182–1201 (2017).
27. **Van Zutphen, T., Todde, V., de Boer, R., Kreim, M., Hofbauer, H. F., Wolinski, H., Veenhuis, M., van der Klei, I. J., and Kohlwein, S. D.:** Lipid droplet autophagy in the yeast *Saccharomyces cerevisiae*, Mol. Biol. Cell, **25**, 290–301 (2014).
28. **Brocard, L., Immel, F., Coulon, D., Esnay, N., Tuphile, K., Pascal, S., Claverol, S., Fouillen, L., Bessoule, J. J., and Brehelin, C.:** Proteomic analysis of lipid droplets from Arabidopsis aging leaves brings new insight into their biogenesis and functions, Front. Plant Sci., **8**, 894 (2017).